Chemical Engineering Journal 164 (2010) 221–229

Contents lists available at ScienceDirect

Chemical Engineering Journal

journal homepage: www.elsevier.com/locate/cej

Prediction of flow behavior of the riser in a novel high solids flux circulating fluidized bed for steam gasification of coal or biomass

Guoqing Guan, Chihiro Fushimi*, Atsushi Tsutsumi*

Collaborative Research Center for Energy Engineering, Department of Mechanical and Biofunctional Systems, Institute of Industrial Science, The University of Tokyo, 4-6-1 Komaba, Meguoro-ku, Tokyo 153-8505, Japan

A R T I C L E I N F O

Article history:
Received 5 April 2010
Received in revised form 30 July 2010
Accepted 2 August 2010

Keywords:
Circulating fluidized bed
High solids mass flux
Pressure balance
Gasification

A B S T R A C T

A triple-bed combined circulating fluidized bed (TBCFB) system, which is composed of a downer, a bubbling fluidized bed (BFB), and a riser, is proposed for the pyrolysis and gasification of coal and biomass. In order to effectively utilize the heat energy produced by the combustion of the char in the riser for the pyrolysis of coal/biomass in the downer and/or gasification of char in the BFB, a high solids mass flux and a large solids holdup are necessary. An analysis of the overall pressure balance around the TBCFB was presented for predicting the maximum achievable solid mass flux under given experimental conditions. The effects of solids inventory, particle physical properties, and gas seal structures on the solids mass flux and the solids holdup were discussed. A correlation for the prediction of solids mass flux in the range of 200–400 kg/m^2 s in the riser under operating conditions was developed based on experimental data from the literature and our laboratory.

1. Introduction

Circulating fluidized bed (CFB) has been investigated extensively for the past several decades due to its added advantages over conventional fluidized bed reactors such as bubbling and turbulent fluidized beds and its widely practical applications in many gas-solid contacting processes such as combustion, coal/biomass gasification and catalytic reactions. Recently, CFBs with high solids mass fluxes ($G_s \geqq 200$ kg/m^2 s) and/or high solids holdups ($\varepsilon_s \geqq 0.1$) were considered as promising equipments for some special processes such as production of maleic anhydride and catalytic cracking of residue/heavy oil which require a higher catalytic/oil ratio [1–6]. In order to differentiate the CFBs operated at low solids fluxes ($G_s < 200$ kg/m^2 s) and/or low solids holdups ($\varepsilon_s < 0.03$), Zhu and Bi [1,2] proposed a concept of “high-density circulating fluidized bed (HDCFB)” and had undertaken a series of studies of HDCFB in their research group [7,8]. Grace et al. [3] named the HDCFB regime as “dense-suspension upflow (DSU)” to represent a CFB condition based on the concept of high-density risers studied by Bi and Zhu, and used the following correlation to describe the transition from the fast fluidization regime to the DSU regime:

$$U_{gr,\mathrm{DSU}} = 0.0113 G_s^{1.192} \rho_g^{-1.064} [\mu_g(\rho_p - \rho_g)]^{-0.064} \quad (1)$$

Table 1 shows the data reported on the CFBs with high solids mass fluxes [9–21]. However, in the riser of these CFB systems, only a few results suggested that a high solids holdup ($\varepsilon_s \geqq 0.1$) was also formed along the entire riser. In general, a dense bottom region ($\varepsilon_s \geqq 0.1$) and a dilute upper region ($\varepsilon_s < 0.05$) were formed along the riser, especially when solid particle with a high density such as sand was used. Wang et al. [12] developed a high solids flux CFB with a Φ0.06 m × 5 m-high riser, and sand particles with a density of 2700 kg/m^3 and an average particle size of 140 μm were used as bed materials. The solids holdup was over 0.1 only below the measured elevation of 1.9 m at the bottom region even when the G_s was over 355 kg/m^2 s. Liu et al. [13] designed a new type CFB by coupling a moving bed to the bottom section of the riser in order to obtain high solids mass fluxes when using sand particles as bed materials. The similar solid holdup distribution in the riser was observed when the G_s was 370 kg/m^2 s. Other experimental investigations on high solids flux CFBs using FCC particles as bed materials also showed the similar characteristics [19–21]. Thus, a high solids flux CFB should not completely equal to a high density CFB. In many cases, DSU and fast fluidization regimes could co-exist in the riser for a given operation condition.

Recently, dual-bed circulating fluidized bed (DBCFB) gasifier, which was proposed in the 1980s, received renewed interest in the high efficiency coal/biomass gasification process for the production of high quality syngas [22–29]. In DBCFB gasifier, coal/biomass can be pyrolyzed/gasified in one bed and the unreacted char is moved to the other bed and combusted in air or pure oxygen flow to generate heat. The produced heat is carried by inert solid particles and moved to the gasifier bed for coal/biomass pyrolysis/gasification.

* Corresponding authors. Tel.: +81 3 5452 6898; fax: +81 3 5452 6728.
E-mail addresses: fushimi@iis.u-tokyo.ac.jp (C. Fushimi), a-tsu2mi@iis.u-tokyo.ac.jp (A. Tsutsumi).

1385-8947/$ – see front matter © 2010 Elsevier B.V. All rights reserved.
doi:10.1016/j.cej.2010.08.005

Table 1
Experimental data with a high solids mass flux in the range of 200–400 kg/m^2 s in the literature.

H_r (m)	D_r (m)	d_p (μm)	ρ_p (kg/m^3)	U_{gr} (m/s)	G_s (kg/m^2 s)	Reference
10.5	0.1	461	2710	10–11.5	200–215	Qi et al. [9]
5.75	0.12	89	2540	5–6	200–250	Mastellone and Arena [10]
10.5	0.4	90	2543	4.9–6	211–264	Arena et al. [11]
5	0.06	140	2700	7.6–10.2	230–395	Wang et al. [12]
12	0.09	378	2600	9.6	370	Liu et al. [13]
15.3	0.1	67	1500	5–10.3	200–230	Qi et al. [9]
10	0.076	67	1500	5.5–10	200–400	Yan and Zhu [14] Pärssinen and Zhu [15]
6.1	0.076	70	1600	4–8	200–400	Issangya et al. [16]
10	0.254	65	1380	7.47	206.3	Ouyang and Potter [17]
7.2	0.076	60	881	4.6	212	Yerushalmi and Cankurt [18]
4.5	0.05	70	1740	7–9	240–360	Kim et al. [19]
5.9	0.203	70	1700	6	250–345	Kim et al. [20]
7	0.14	89	1740	4.7	229–264	Malcus et al. [21]
6	0.05	83	2600	5–8	200–333	This work

In order to use the heat efficiently, DBCFB gasifier should be operated at a high solids mass flux [30,31]. On the other hand, when the pyrolysis and gasification were carried out at the same bed, the produced tar, light hydrocarbon gases and inorganic gases at the initial coal/biomass pyrolysis stage could severely hinder the gasification of the char [32–34]. Thus, in order to maintain the catalyst activity and/or to enhance the efficiency of char gasification, the produced volatiles in pyrolysis stage should be separated with the remaining char. In our study, a triple-bed combined circulating fluidized bed (TBCFB) system, which is composed of a downer, a bubbling fluidized bed (BFB), and a riser, is proposed. The coal/biomass is pyrolyzed rapidly in the downer at first, and then, the obtained gas and tar are separated from the char using a gas-solid separator. The char enters the BFB to be gasified with the steam in a relatively long residence time. The unreacted char is moved into the riser and partially or completely oxidized with oxygen or air. The produced heat is also carried by inert solid medium such as sand, and circulated into the downer and the BFB to provide the heat needed in the pyrolysis and gasification processes. In order to effectively utilize the heat energy produced by the combustion of the char in the riser for the pyrolysis of coal/biomass in the downer and/or steam gasification of char in the BFB, a high solids mass flux and a large solids holdup are also required in this system. In the present study, such a TBCFB coal/biomass gasifier cold model was set up, and the flow behaviors were investigated. In order to predict the maximum achievable solid mass flux under given experimental conditions, the overall pressure balance around the TBCFB was analyzed. A correlation for the prediction of high solids mass flux in the riser under operating conditions was obtained based on experimental data from the literature and our experiments.

2. Experimental

As shown in Fig. 1, the TBCFB experimental system is composed of an acrylic riser (0.05 m-I.D. × 6 m-high), a solid distributor for downer, a downer (0.1 m-I.D. × 1.3 m), a gas-solid separator, and a BFB (0.37 m × 0.08 m × 1.5 m). When a practical TBCFB gasifier is designed, gas seal, which controls the flow of particles from one bed to the other while prevents the gas from intermixing between the beds, should be considered [27,28]. In this TBCFB cold model, as suggested by Xu et al. [27], the seal structure between the BFB and the riser (seal BR) was designed as a siphon, and the seal between the downer and the BFB (seal DB) was performed by inserting the dipleg (0.05 m-I.D. × 0.65 m) of gas-solids separator into the BFB. The seal between the riser and the downer (seal RD) was realized by adjusting the openness of a mechanical valve to form a moving bed layer which blocks the gas from the riser to the downer but keeps the particles freely flowing into the downer. Two kinds of sand particles with a density of 2600 kg/m^3 and average particle sizes of 83 (terminal velocity U_t = 0.4354 m/s) and 320 μm (U_t = 2.403 m/s), respectively, were used as bed materials. During the operation, solids from the BFB passed through the seal BR and flowed into the riser, and then, were carried upwards by air along the riser tube. At the top of the riser, the solids passed through a smooth elbow into a cyclone for gas-solid separation. At the top of the downer, the solids passed through the seal RD and were redis-

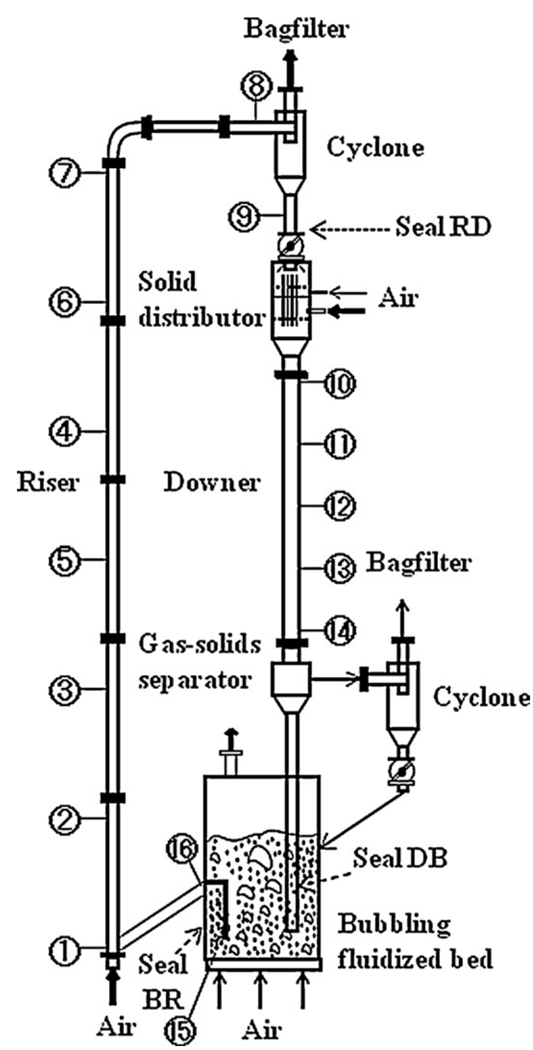

Fig. 1. Schematic diagram of the experimental apparatus.

tributed by a solids distributor located below the seal RD. The solids were overflow into 7 vertically positioned brass tubes with an inner diameter of 15 mm with the assistance of minimum fluidization gas. The downward flow air was introduced into the downer at the entrance of the downer. The co-current down-flow gas-solid flowed down along the downer, and at the end of the downer, the solids were separated from the gas by a quick inertial separator with an efficiency of more than 96% and returned to the BFB through the seal DB. The solids entrained by the gas at the gas-solids separator was further separated by a cyclone and returned to the BFB. The superficial gas velocities of the riser and the downer ranged from 3 to 8 m/s and from 0 to 5 m/s, respectively, but that of BFB (U_b) was fixed at $5 \times U_{\rm mf}$. 16 pressure taps were installed along the TBCFB systems as shown in Fig. 1 and differential pressure sensors (Keyence Corp., AP48) were used. The output signals from the differential pressure sensors were acquired at a sampling frequency of 50 Hz via a data acquisition system (CONTEC, AIO-163202FX) and a laptop computer. When wall friction and solids acceleration are neglected, the apparent solids holdup can be determined by measuring the average differential pressures across the sections of the bed and equating the static pressure drop to the bulk weight in the bed sections, i.e.

$$\frac{\Delta P}{\Delta H} = \rho_p \varepsilon_s g + \rho_g (1-\varepsilon_s) g \tag{2}$$

As reported in the literature [4–9,12–16], solids mass flux (G_s) was measured using a butterfly valve with amounts of accumulated particles for a given time period within several seconds, and determined from the mean value with 10 times measurements at steady state. It should be noted that the real G_s should be greater than the measured one using this method.

3. Pressure balance of the TBCFB loop

The TBCFB system shown in Fig. 1 was represented in a simple manner as illustrated in Fig. 2 in order to analyze the pressure balance along it. In the present model, the pressures at the exit of the cyclone of the riser, the outlet of the gas-separator of the downer, and the upper zone of BFB can be taken as reference pressures since they were opened to the air, i.e.,

$$P_c = P_s = P_f \tag{3}$$

Thus, the stable circulating of the solids in this TBCFB system is mainly determined by the pressure balance between the riser and the BFB.

In a stable operation, the surface of the seal DB can be considered as the same level of that of the BFB. The solids holdup in the seal DB (ε_{db}) can be assumed to be the same as that in the seal BR (ε_{br}), i.e.,

$$\varepsilon_{db} = \varepsilon_{br} = \varepsilon_{seal} \tag{4}$$

Furthermore, the exit effect of the seals and the effect of particles existed in the space above the moving bed seal in the dipleg of the gas-solids separator on the pressure balance between the riser and the BFB are neglected. Since the gas velocity and particle moving velocity in the BFB as well as in the seal are relatively low, pressure drops caused by gas-wall friction and particle-wall friction are also neglected. Based on these assumptions, the pressure head at the exit of the seal BR to the riser can be calculated by:

$$\begin{aligned} P_d = & [\rho_p \varepsilon_{seal} + \rho_g (1-\varepsilon_{seal})] g (H_{db} - H_{br}) \\ & + [\rho_p \varepsilon_{sb} + \rho_g (1-\varepsilon_{sb})] g (H_{\rm BFB} - H_{db}) \end{aligned} \tag{5}$$

where $H_{\rm BFB}$ is the height of bubbling fluidized bed at an operation state. Since the cross area of the BFB is much larger than those of the riser and the downer, $H_{\rm BFB}$ can be assumed as a constant during the operation for a fixed solids inventory.

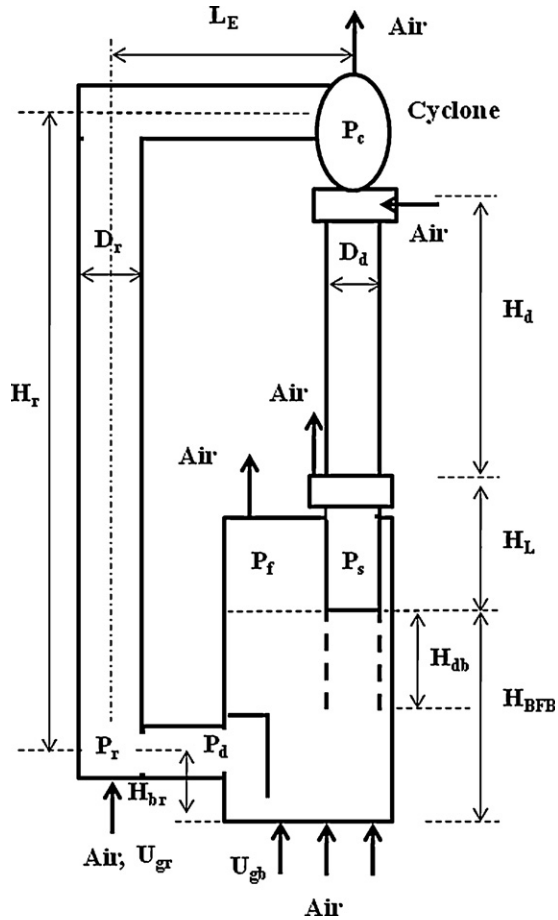

Fig. 2. Pressure balance of the TBCFB system.

According to our previous experimental study [35] and the results in the literature [9–21], a relatively dense solids phase generally formed at the bottom of the riser while a dilute solids phase formed in the upper area even when the solids mass flux was over 350 kg/m^2 s. Thus, the riser is axially divided into the lower dense area and the upper dilute area in this model. Many correlations for estimating solids holdup along the riser are available in the literature [36,37]. Regarding to the riser operated at a high solids mass flux, Bai and Kato [36] developed general correlations to prediction of solids holdups at the dense and dilute areas, which have been identified to be applicable in a wide range of operating conditions [36–38]. Based on these assumptions, the pressure head at the bottom of the riser, P_r, can be calculated by:

$$\begin{aligned} P_r = & [\rho_s \varepsilon_{s,den} + \rho_g (1-\varepsilon_{s,den})] g h_{den} + [\rho_s \varepsilon_{s,dil} + \rho_g (1-\varepsilon_{s,dil})] g h_{dil} \\ & + \Delta P_c + \Delta P_{fg} + \Delta P_{fs} + \Delta p_{ac} \end{aligned} \tag{6}$$

where $\varepsilon_{s,den}$ and $\varepsilon_{s,dil}$ are average solids holdups in the dense and in the dilute phase areas of the riser, respectively, and can be estimated by the following equations [36]:

$$\varepsilon_{s,den} = \left[1 + 0.103 \left(\frac{\rho_p U_{gr}}{G_s} \right)^{1.13} \left(\frac{\rho_p - \rho_g}{\rho_g} \right)^{-0.013} \right] \varepsilon^* \tag{7}$$

$$\varepsilon_{s,dil} = \left[1 + 0.208 \left(\frac{\rho_p U_{gr}}{G_s} \right)^{0.5} \left(\frac{\rho_p - \rho_g}{\rho_g} \right)^{-0.082} \right] \varepsilon^* \tag{8}$$

where

$$\varepsilon^* = \frac{G_s}{\rho_p(U_{gr} - U_t)} \quad (9)$$

h_{den} and h_{dil} in Eq. (6) are the heights of the dense and the dilute phase sections respectively, and can be calculated using the following equations [39]:

$$h_{den} = 360\left(\frac{G_s}{\rho_p U_t}\right)^{1.2}\left(\frac{U_{gr} - U_t}{U_t}\right)^{-1.45}]\ \mathrm{Re}_p^{-0.29} \quad (10)$$

where

$$\mathrm{Re}_p = \frac{d_p U_{gr}\rho_g}{\mu_g} \quad (11)$$

and

$$h_{dil} = h_r - h_{den} \quad (12)$$

The pressure drops, ΔP_c, ΔP_{fg}, ΔP_{fs}, and Δp_{ac} are the cyclone pressure drop, the pressure drop due to gas-wall friction, the pressure drop due to particle-wall friction, and the pressure drop due to particle acceleration, respectively. The amount of solids held in the cyclone could be neglected, and the pressure drop over the cyclone is assumed to be dependent on the gas velocity. Thus, the pressure drop across the cyclone can be estimated by [7]:

$$\Delta P_c = k\rho_g U_{cy}^2 \quad (13)$$

where k is depended on the cyclone structure. For CFB cyclone, it is recommended that U_{cy} can be taken as the superficial gas velocity of the riser (U_{gr}) and $k = 25$ [1,7,38].

The solids holdup in the connection tube between the riser and the cyclone is assumed to be the same as that in the upper area of the riser. Then, the pressure drop due to gas-wall friction can be estimated by Fanning equation as following [7]:

$$\Delta P_{fg} = 2f_g(1 - \varepsilon_{s,den})\rho_g U_{gr}^2\left(\frac{h_{den}}{D_r}\right) + 2f_g(1 - \varepsilon_{s,dil})\rho_g U_{gr}^2\left(\frac{h_{dil} + L_E}{D_r}\right) \quad (14)$$

where

$$f_g = \frac{0.079}{\mathrm{Re}^{0.313}}, \quad \mathrm{Re} = \frac{D_r U_{gr}\rho_g}{\mu_g} > 2300 \quad (15)$$

$$f_g = \frac{16}{\mathrm{Re}}, \quad \mathrm{Re} \leqq 2300 \quad (16)$$

In general, pressure drop due to gas-wall friction is usually a relatively minor component in the whole pressure balance. Thus, we also used this simple approach here.

The pressure drop due to particle-wall friction can be calculated by the equation proposed by Konno and Saito [40],

$$\Delta P_{fs} = 0.057g(H_r + L_E)\frac{G_s}{\sqrt{gD_r}} \quad (17)$$

which is generally used for the riser.

The pressure drop due to the particle acceleration is generally estimated by [7]

$$\Delta P_{ac} = \frac{G_s^2}{\varepsilon_{s,ave}\rho_s} \quad (18)$$

Here, the following equation to calculate $\varepsilon_{s,ave}$ is used in this model

$$\varepsilon_{s,ave} = \frac{\varepsilon_{s,den}h_{den} + \varepsilon_{s,dil}h_{dil}}{h_{den} + h_{dil}} \quad (19)$$

For the present TBCFB system, no solids control valve is set between the BFB and the riser. Under steady state operation, P_d can be considered to be equal to P_r in order to maintain a pressure balance in the entire loop, i.e.,

$$P_d = P_r \quad (20)$$

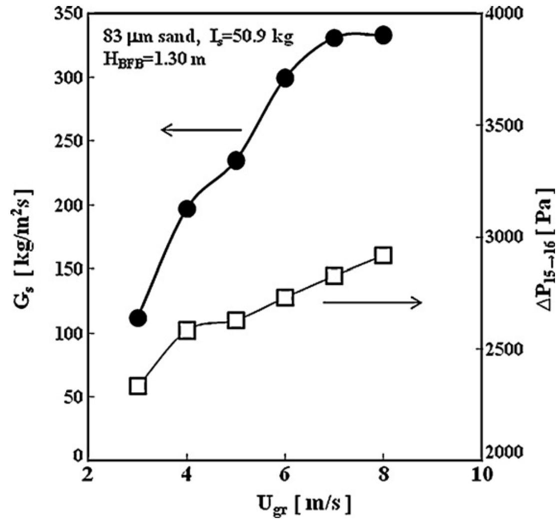

Fig. 3. Relationship of G_s and the pressure difference between the bottom of BFB and the exit of seal RB to riser.

As indicated in Fig. 3, in our experimental system, the force pushing the particle to flow into the riser from the BFB depends on the pressure difference between the bottom of the BFB (point 15) and the exit of seal BR (Point 16) to the riser, and P_d (Point 16) also approximately equals to P_r (Point 1) [35].

4. Results and discussion

4.1. Effect of BFB height on the solids mass flux

The achievable solids mass flux at a given riser gas velocity (U_{gr}) can be predicted according to the above pressure balance model. Fig. 4 shows the effect of the BFB height (H_{BFB}) at a fixed operation condition (U_{gb} = 0.3 m/s) on the solids mass flux. At a given U_{gr}, the solids mass flux obviously increases with the increase in the BFB height, suggesting that H_{BFB} has a great effect on G_s. It should be noted H_{BFB} at a fixed operation condition increases with the

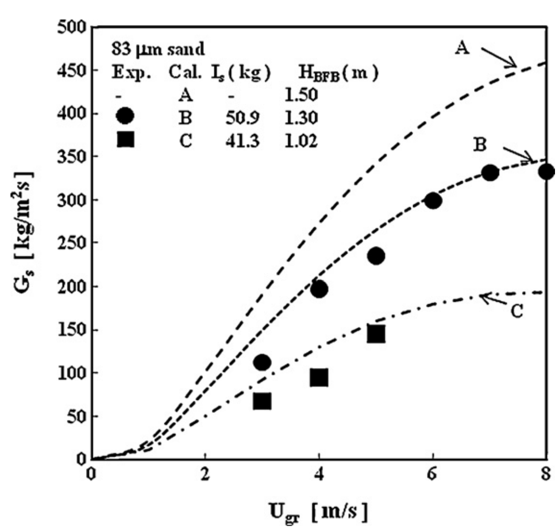

Fig. 4. Effect of the gas velocity in the riser on solids mass flux with different solids inventory in the TBCFB system.

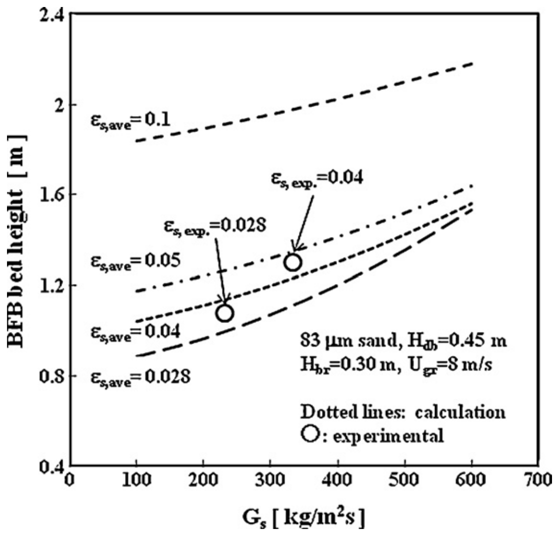

Fig. 5. A prediction study if the whole riser worked at a constant solids holdup in the TBCFB system.

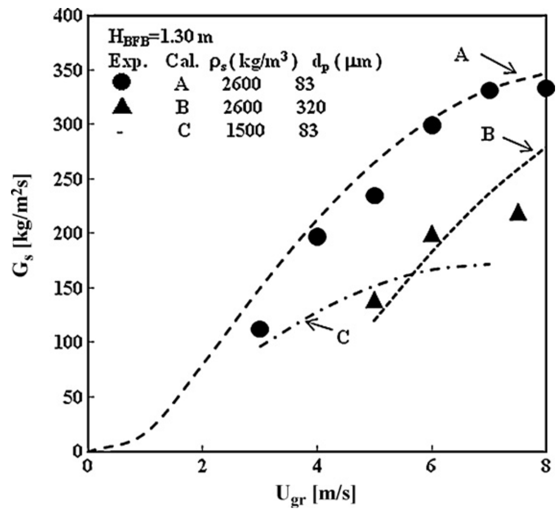

Fig. 6. Effects of particle size and density on solids mass flux.

increase in total solids inventory (I_s). As shown in Fig. 4, experimental results also indicate that the G_s increases with the increase in H_{BFB}. Therefore, for a TBCFB system, in order to get a higher G_s, a larger amount of I_s is necessary. On the other hand, for each H_{BFB} in Fig. 4, predicted G_s increases quickly with increasing riser gas velocity at low U_{gr}, whereas little change is predicted at high U_{gr}. It suggests that the solids mass flux could be restricted by the solids feeding ability from the BFB to the riser at high U_{gr}. In the present system, this solid feeding ability depends on the pressure head at the bottom of the BFB when the seal BR height (H_{br}) is fixed. However, the pressure head should be limited when G_s increased beyond a certain value for a given BFB height so that no enough solids feed into the riser. Bi and Zhu [1] set up a pressure balance model for a CFB system composed of a riser, a downcomer and a solids control valve between them, and a similar phenomenon was also observed. As shown in Fig. 4, the experimental results also indicated this trend. Although the TBCFB system was simplified in order to obtain the pressure balance model and some empirical equations were used in the pressure balance model, the prediction result is seen to be in good agreement with the experimental data. Moreover, it should be noted that the calculated solids flux via the pressure balance is the maximum value corresponding to the given gas velocity in the riser [1,7].

Our previous study suggested that the steam gasification of coal and biomass in a DBCFB system should be operated in a high solids mass flux and a high solids holdup in order to supply sufficient heat to the endothermic steam gasification reaction [31]. The same requirements should be also necessary for a TBCFB system design. As discussed above, almost all studies reported were performed at a low-density riser with a particle flow structure having a dense phase at bottom and a relatively dilute phase in the top section even at a high solids mass flux state, mainly due to the restriction on the solids feeding system for riser. As for the present TBCFB system, the force pushing the particles to flow into the riser depends on the BFB height. In order to predict the required H_{BFB} when the riser of such a TBCFB system could be operated at a high density state such as average solid holdup ($\varepsilon_{s,ave}$) = 0.1, a case study assuming $\varepsilon_{s,den} = \varepsilon_{s,dil}$ = (a constant) in the pressure balance model was performed. The obtained relationships of G_s and H_{BFB} at a fixed $\varepsilon_{s,ave}$ in the riser are shown in Fig. 5. It can be seen that H_{BFB} should be greater than 1.90 m when U_{gr} is 8.0 m/s for the present riser if it could be operated in a state with a high G_s (G_s > 200 kg/m^2 s) as well as a high $\varepsilon_{s,ave}$ ($\varepsilon_{s,ave}$ > 0.1). However, the maximum BFB solids height in the present experimental system was approximately 1.3 m at U_{BFB} = 0.03 m/s, and the obtained average solids holdup ($\varepsilon_{s,exp.}$) was only approximately 0.04 although G_s was 333 kg/m^2 s. On the other hand, it can be seen that G_s should reach 395 kg/m^2 s according to the present model if $\varepsilon_{s,ave}$ in the riser is assumed to be 0.04 when H_{BFB} = 1.3 m and U_{gr} = 8 m/s. The deviation of this calculation and the experimental result is approximately 15.7%, suggesting that the prediction results are believable. This result could provide the guidance for a possible high-density TBCFB system design.

4.2. Effects of solids physical properties on the solids mass flux

According to the pressure balance model, the particle physical properties such as particle size and density should have great influence on the solids mass flux. Fig. 6 shows the effects of solid average size (d_p) and density (ρ_p) on G_s under the same operation conditions. It can be seen that G_s decreased with the increase in d_p whereas increased with the increase in ρ_p. The experimental results also show that the G_s reached 333 kg/m^2 s for 83 µm sand but only 220 kg/m^2 s for 320 µm sand at U_{gr} = 8 m/s. As indicated in Table 1, high solids mass flux is generally achievable for relatively fine particles. Chen et al. [38] reported that the heavier particles gave a higher G_s in a CFB system composed of a riser, a downer and a solids control valve between them under a same operation condition. On the other hand, according to the pressure balance model, selecting a particle such as glass beads or FCC particles with good fluidity could increase the G_s by decreasing particles-wall friction in the riser.

4.3. Effects of gas seals on the solids mass flux

The effects of the similar gas seals DB and BR on solids mass flux in a DBCFB system with G_s lower than 25 kg/m^2 s have been experimentally investigated by Xu et al. [27]. In their case, the length of seal DR inserting into the BFB had no effect on the solids mass flux. However, it is found that the whole system cannot be operated at a high G_s (for example, G_s > 140 kg/m^2 s) in our TBCFB system if a long inserted seal DR tube was used [35]. This may result from the high resistance of particles flow in the long seal tube, which could slow down the particle moving rate and form a bottleneck for particle flow from downer to BFB at high G_s conditions. According to the above pressure balance model, the effect of the seal DB heights (H_{db}) on G_s was predicted. As shown in Fig. 7, G_s increases to some extent

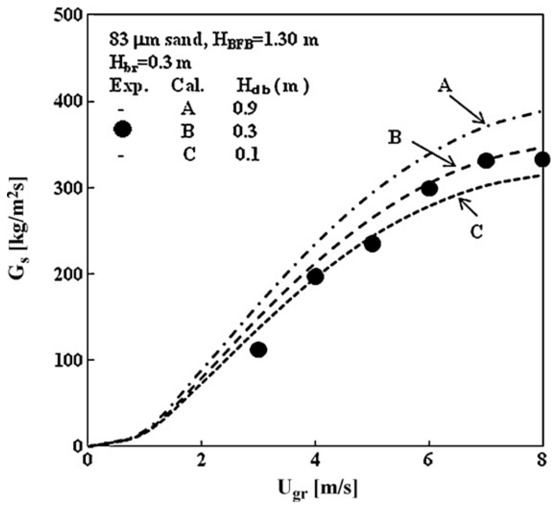

Fig. 7. Effect of seal DB height on solids mass flux.

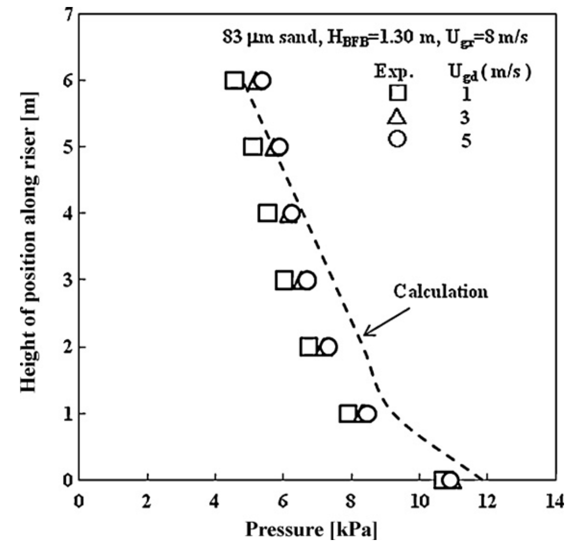

Fig. 9. Prediction of pressure distribution in the riser.

when a higher H_{db} is used. However, as stated above, the negative effect of a high H_{db} should be considered for a high solids mass flux TBCFB system design. In the present experimental study, H_{db} was 0.45 m when H_{BFB} = 1.30 m, and it is found that the whole system was operated stably even at a condition of G_s over 330 kg/m^2 s. In this case, the effect of the height of the seal BR (H_{br}) between the BFB and the riser was also predicted. As shown in Fig. 8, H_{br} has greater influence on G_s than H_{db}. As the H_{br} decreases, G_s increases. However, the gas seal function could lose if H_{br} is designed too low.

In this study, the gas seal between the riser and the downer (seal RD) was realized by adjusting the openness of a mechanical valve to form a moving bed layer between the cyclone and the downer. The effect of the seal RD on the pressure distribution along the downer was investigated in our previous study [35]. It is found that the pressure distributions along the downer with the seal RD was different from those without the seal, and the static pressure at any point decreased to some extent due to the seal RD. The entering of the gas from the riser into the downer with the particle flow in the non-seal state resulted in the increasing of the static pressure in the downer. On the other hand, as shown in Figs. 9 and 10, the experimental results indicate that the pressure distribution and solids holdup distribution along the riser almost keep unchangeable with increasing gas velocity in the downer (U_{gd}). This should be attributed to the gas seal functions of seal RB, DB and BR. Therefore, it is reasonable to assume that the pressure drop in the downer has no effect on the pressure balance between the riser and the BFB. The profiles of pressure and solids holdup along the riser were predicted by the pressure balance model, which is almost validated with the experimental data as indicated in Figs. 9 and 10.

4.4. Empirical correlation on G_s prediction

G_s and U_{gr} are two important variables to describe the flow behavior of CFB [3,41]. Various attempts have been made to obtain the flow regime maps of gas solids flow system in which solids mass flux was plotted against superficial gas velocity [3,42,43]. Bi and Fan [42] originally proposed the following Eq. (21) to predict the so-called saturation carrying capacity to feature the regime transition between core-annular dilute-phase gas-solids flow and fast fluidization at low G_s conditions.

$$\frac{U_{gr}}{\sqrt{gd_p}} = 21.6Ar^{0.105}\left(\frac{G_s}{\rho_g U_{gr}}\right)^{0.542} \quad (21)$$

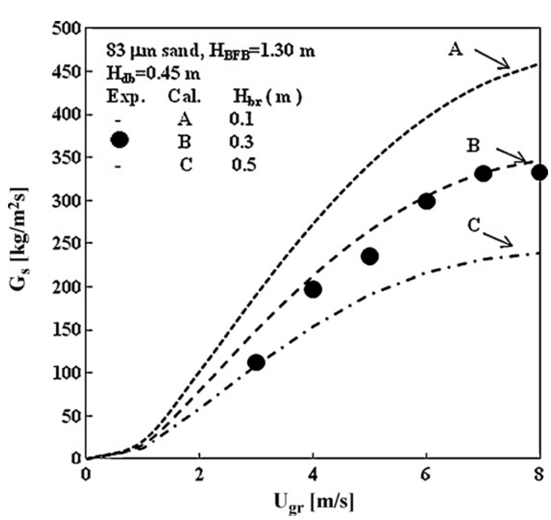

Fig. 8. Effect of seal BF height on solids mass flux.

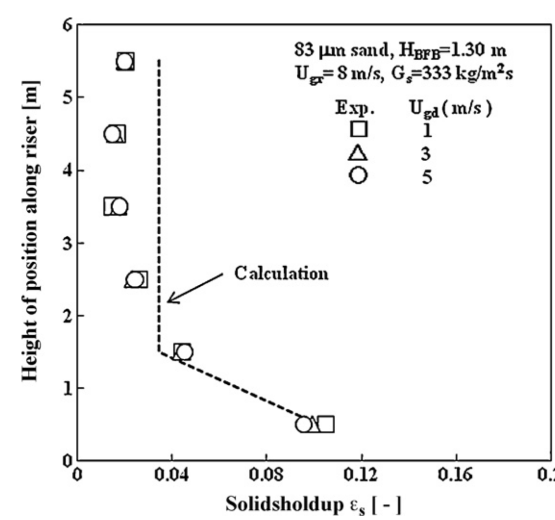

Fig. 10. Prediction of solids holdup in the riser.

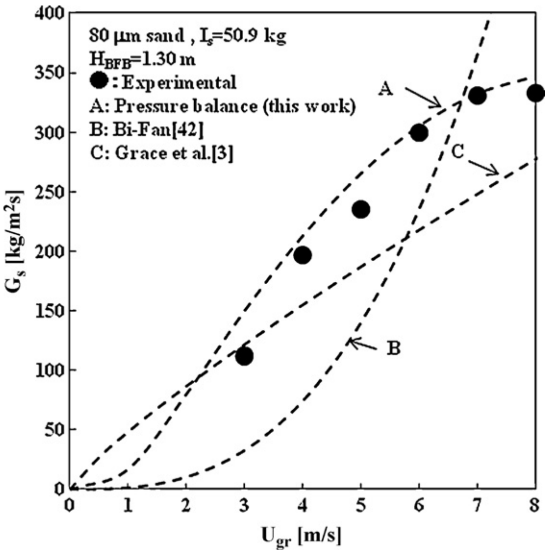

Fig. 11. The flow regimes of the riser in the TBCFB system.

Grace et al. used Eq. (1) to describe the transition from the fast fluidization regime to the DSU regime [3]. Fig. 11 shows the results when the two equations were used for the present system. According to Eq. (21), when $U_{gr} < 7$ m/s, the riser was operated in a state beyond the point of the saturation carrying capacity and below the predicted maximum solids mass flux. However, when $U_{gr} > 7$ m/s, the riser was still operated in a dilute-phase flow state, suggesting that a higher solids mass flux could be reached if enough solids can be feed from BFB to the riser. As stated above, to achieve higher G_s at a high U_{gr}, the best way is to increase H_{BFB} for this system. On the other hand, it can be seen that Eq. (1) cannot be used to predict the onset of the DSU regime of the present system. Eq. (1) should only be valid in the operation conditions where it was obtained: $\varepsilon_s \geqq 0.07$; $7 \leqq G_s/\rho_g U_{gr} \leqq 100$; $51\ \mathrm{mm} \leqq D_r \leqq 305\ \mathrm{mm}$; and $6.1\ \mathrm{m} \leqq H_r \leqq 27.4\ \mathrm{m}$.

Although a high G_s is urgently expected for some industrial process, only a few data on $G_s > 400\ \mathrm{kg/m^2\,s}$ was reported in the literature [14,44,45]. If variables like riser diameter and height, gas and solids physical properties are considered, G_s in the riser should be a function of seven variables, that is,

$$G_s = f(U_{gr}, d_p, \rho_p, \rho_g, \mu_g, D_r, H_r) \tag{22}$$

which can be expressed by four dimensionless parameters, i.e. $G_s d_p/\mu_g$, Ar, $U_{gr}/(gD_r)^{1/2}$, and D_r/H_r. Based on the experimental data obtained in the literature and in the present study for the CFB risers with a solids mass flux between 200 and 400 kg/m² s as indicated in Table 1, the following correlation is obtained to correlate the solids mass flux and operation conditions:

$$\frac{G_s d_p}{\mu_g} = 547 Ar^{0.248} \left(\frac{U_{gr}}{\sqrt{gD_r}} \right)^{0.375} \left(\frac{D_r}{H_r} \right)^{0.195} \tag{23}$$

The data leading to this equation cover the range of variables: $0.05\ \mathrm{m} \leqq D_r \leqq 0.4\ \mathrm{m}$, $60\ \mu\mathrm{m} \leqq d_p \leqq 461\ \mu\mathrm{m}$, $881\ \mathrm{kg/m^3} \leqq \rho_p \leqq 2710\ \mathrm{kg/m^3}$, $4.6\ \mathrm{m/s} \leqq U_{gr} \leqq 11.5\ \mathrm{m/s}$, and $200\ \mathrm{kg/m^2\,s} \leqq G_s \leqq 400\ \mathrm{kg/m^2\,s}$. A comparison between the calculated values of Eq. (23) and the experimental data showed in Table 1 and obtained in the present study is shown in Fig. 12. It can be seen that the predictions of the correlation fit well with the experimental data obtained from this work and in the literature with a relative deviation of less than 25%.

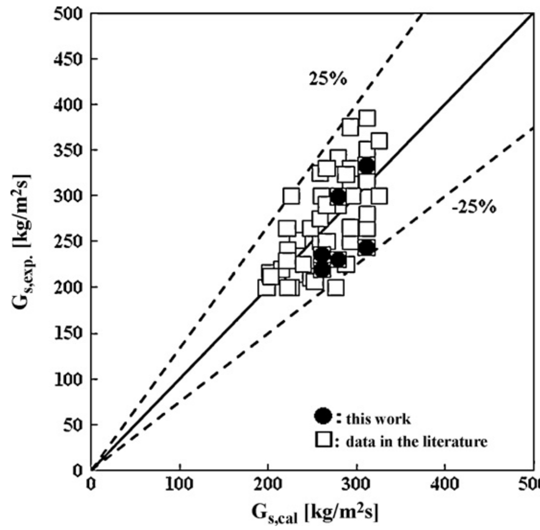

Fig. 12. Comparison of the calculated values of Eq. (23) and the experimental data.

5. Conclusions

The overall pressure balance analysis around the triple-bed combined circulating fluidized bed system was performed for predicting the maximum achievable solids flux under given experimental conditions. The general trend of the model is seen to be in good agreement with the experimental data. The effects of solids inventory, particle physical properties and seal structures on the solids mass flux were also predicted and discussed. In order to obtain a higher solids mass flux and a higher density in TBCFB system, the best way is to add more particles into the system. In additions, fine particles with a high density are also benefit for a TBCFB system with a high solids mass flux and/or a high density. The heights of gas seal DB and BR should be designed carefully to guarantee a particle flow with a high solids mass flux to pass through them smoothly. Based on the numerous experimental data from CFB risers, an empirical correlation for the prediction of high solids mass fluxes ($200 \leqq G_s \leqq 400\ \mathrm{kg/m^2\,s}$) in the riser is proposed.

List of symbols

Ar	Archimedes number $(= d_p^3 \rho_g g(\rho_p - \rho_g)/\mu_g^2)$
D_d	downer internal diameter (m)
D_r	riser internal diameter (m)
d_p	average diameter of particles (m)
f_g	gas-wall friction coefficient
f_s	solids-wall friction coefficient
g	acceleration due to gravity (m/s²)
G_s	solids mass flux (kg/m² s)
$G_{s,\mathrm{cal}}$	calculated solids mass flux (kg/m² s)
$G_{s,\mathrm{exp.}}$	experimental solids mass flux (kg/m² s)
h_{den}	height of dense phase section of riser (m)
h_{dil}	height of dilute phase section of riser (m)
H_{BFB}	height of bubble fluidized bed (m)
H_{br}	height of the seal between bubbling fluidized bed and riser (m)
H_{db}	height of the seal between downer and bubbling fluidized bed (m)
H_d	downer height (m)
H_L	height between gas-solids separator and the surface of bubbling fluidized bed (m)
H_r	riser height (m)
I_s	solids inventory (kg)
L_E	elbow length (m)
P_c	pressure head at exit of the cyclone (Pa)

P_d	pressure head at the exit of the BFB to riser (Pa)
P_f	pressure head at the top of the BFB (Pa)
P_r	pressure head at the bottom of riser (Pa)
P_s	pressure head at exit of the gas-solid separator (Pa)
ΔP_{ac}	pressure drop due to solids acceleration (Pa)
ΔP_c	pressure drop across cyclone (Pa)
ΔP_{fg}	pressure drop due to gas-wall friction (Pa)
ΔP_{fs}	pressure drop due to solids-wall friction (Pa)
Re	Reynolds number ($=D_r U_{gr} \rho_g/\mu_g$)
Re_p	Reynolds number ($=d_p U_{gr} \rho_g/\mu_g$)
U_{gb}	superficial gas velocity in the bubbling fluidized bed (m/s)
U_{gd}	superficial gas velocity in the downer (m/s)
U_{gr}	superficial gas velocity in the riser (m/s)
U_t	terminal velocity of a single particle (m/s)

Greek letters

ρ_g	gas density (kg/m^3)
ρ_p	particle density (kg/m^3)
ε_s	solids holdup in the riser
$\varepsilon_{s,ave}$	average solids holdup in the riser
$\varepsilon_{s,den}$	solids holdup at dense phase section in the riser
$\varepsilon_{s,dil}$	solids holdup at dilute phase section in the riser
$\varepsilon_{s,\mathrm{exp.}}$	experimental value of average solids holdup in the riser
ε_{sb}	solids holdup in BFB
μ_g	gas viscosity (Pa s)

Abbreviation list

BFB	bubbling fluidized bed
BR	bubbling fluidized bed-riser
Cal.	calculation
CFB	circulating fluidized bed
DBCFB	dual-bed circulating fluidized bed
DB	downer-bubbling fluidized bed
DSU	dense-suspension upflow
Exp.	experimental
HDCFB	high density circulating fluidized bed
RD	riser–downer
TBCFB	triple-bed circulating fluidized bed

Acknowledgements

This study is supported by the New Energy and Industrial Technology Development Organization (NEDO). The authors thank Dr. Masahiro Ikeda, Mr. Masanori Ishizuka and Mr. Yu Nakamura for their technical support.

References

[1] H.-T. Bi, J. Zhu, Static instability analysis of circulating fluidized beds and concept of high-density risers, AIChE J. 39 (1993) 1272–1280.
[2] J.-X. Zhu, H.-T. Bi, Distinctions between low density and high density circulating fluidized beds, Can. J. Chem. Eng. 73 (1995) 644–649.
[3] J.R. Grace, A.S. Issangya, D. Bai, H.-T. Bi, J.-X. Zhu, Situating the high-density circulating fluidized bed, AIChE J. 45 (1999) 2108–2116.
[4] J.H. Pärssinen, J.-X. Zhu, Axial and radial solid distribution in a long and high-flux CFB riser, AIChE J. 47 (2001) 2197–2205.
[5] F. Wei, F. Lu, Y. Jin, Z. Yu, Mass flux profiles in a high density circulating fluidized bed, Powder Technol. 91 (1997) 189–195.
[6] F. Wei, H. Lin, Y. Cheng, Z. Wang, Y. Jin, Profiles of particle velocity and solids fraction in a high-density riser, Powder Technol. 100 (1998) 183–189.
[7] D. Bai, A.S. Issangya, J.-X. Zhu, J.R. Grace, Analysis of the overall pressure balance around a high-density circulating fluidized bed, Ind. Eng. Chem. Res. 36 (1997) 3898–3903.
[8] A.S. Issangya, J.R. Grace, D. Bai, J.-X. Zhu, Further measurements of flow dynamics in a high-density circulating fluidized bed riser, Powder Technol. 111 (2000) 104–113.
[9] X.-B. Qi, J. Zhu, W.-X. Huang, A new correlation for predicting solids concentration in the fully developed zone of circulating fluidized bed risers, Powder Technol. 188 (2008) 64–72.
[10] M.I. Mastellone, U. Arena, The effect of particle size and density on solids distribution along the riser of a circulating fluidized bed, Chem. Eng. Sci. 54 (1999) 5383–5391.
[11] U. Arena, A. Malandrino, L.A. Marzocchella, L. Massimilla, Flow structure in the risers of laboratory and pilot CFB units, in: P. Basu, M. Horio, M. Hasatani (Eds.), Circulating Fluidized Bed Technology, vol. III, Pergamon Press, Toronto, 1991, pp. 137–144.
[12] X. Wang, B. Jin, W. Zhong, M. Zhang, Y. Huang, F. Duan, Flow behaviors in a high-flux circulating fluidized bed, Int. J. Chem. Reaction Eng. 6 (2008) (Article A79).
[13] X. Liu, X. Cui, G. Sun, G. Sun, T. Suda, G. Xu, High solid-flux concurrent conveying flow realized by coupling a moving bed to the bottom section of a riser, Ind. Eng. Chem. Res. 47 (2008) 9703–9708.
[14] A.-J. Yan, J.-X. Zhu, Scale-up effect of riser reactors (1): axial and radial solids concentration distribution and flow development, Ind. Eng. Chem. Res. 43 (2004) 5810–5819.
[15] J.H. Pärssinen, J.-X. Zhu, Particle velocity and flow development in a long and high-flux circulating fluidized bed riser, Chem. Eng. Sci. 56 (2001) 5295–5303.
[16] A.S. Issangya, D. Bai, H.T. Bi, K.S. Lim, J. Zhu, J.R. Grace, Suspension densities in a high-density circulating fluidized bed riser, Chem. Eng. Sci. 54 (1999) 5451–5460.
[17] S. Ouyang, O.E. Potter, Consistency of circulating fluidized bed experimental data, Ind. Eng. Chem. Res. 32 (1993) 1041–1045.
[18] J. Yerushalmi, N.T. Cankurt, Further studies of the regimes of fluidization, Powder Technol. 24 (1979) 187–205.
[19] J.-S. Kim, R. Tachino, A. Tsutsumi, Effects of solids feeder and riser exit configuration on establishing high density circulating fluidized beds, Powder Technol. 187 (2008) 37–45.
[20] S.W. Kim, G. Kirbas, H. Bi, C.J. Lim, J.R. Grace, Flow behavior and regime transition in a high-density circulating fluidized bed riser, Chem. Eng. Sci. 59 (2004) 3955–3963.
[21] S. Malcus, E. Cruz, C. Rowe, T.S. Pugsley, Radial solid mass flux profiles in a high-suspension density circulating fluidized bed, Powder Technol. 125 (2002) 5–9.
[22] J. Corella, J.M. Toledo, G. Molina, A review on dual fluidized-bed biomass gasifier, Ind. Eng. Chem. Res. 46 (2007) 6831–6839.
[23] K. Kuramoto, K. Matsuoka, T. Murakami, H. Takagi, T. Nanba, Y. Suzuki, S. Hosokai, J.-i. Hayashi, Cracking and coking behaviors of nascent volatiles derives from flash pyrolysis of woody biomass over mesoporous fluidized-bed material, Ind. Eng. Chem. Res. 48 (2009) 2851–2860.
[24] S. Hosokai, M. Sugawa, K. Norinaga, C.-Z. Li, J.-i. Hayashi, Activity of mesoporous alumina particles for biomass steam reforming in a fluidized-bed reactor and its application to a dual-gas-flow two-stage reactor system, Ind. Eng. Chem. Res. 47 (2008) 5346–5352.
[25] K. Matsuoka, K. Kuramoto, T. Murakami, Y. Suzuki, Steam gasification of woody biomass in a circulating dual bubbling fluidized bed system, Energy Fuels 22 (2008) 1980–1985.
[26] L. Wei, S. Xu, J. Liu, C. Lu, S. Liu, C. Liu, A novel process of biomass gasification for hydrogen-rich gas with solid heat carrier: preliminary experimental results, Energy Fuels 20 (2006) 2266–2273.
[27] G. Xu, T. Murakami, T. Suda, Y. Matsuzawa, Reactor siphon and its control of particle flow rate when integrated into a circulating fluidized bed, Ind. Eng. Chem. Res. 44 (2005) 9347–9354.
[28] G. Xu, T. Murakami, T. Suda, Y. Matsuzawa, H. Tani, Particle circulation rate in high-temperature CFB: measurement and temperature influence, AIChE J. 52 (2006) 3626–3630.
[29] G. Xu, T. Murakami, T. Suda, Y. Matsuzawa, H. Tani, The superior technical choice for dual fluidized bed gasification, Ind. Eng. Chem. Res. 45 (2006) 2281–2286.
[30] X.T. Bi, X. Liu, High density and high solids flux CFB risers for steam gasification of solids fuels, Fuel Process. Technol. 91 (2010) 915–920.
[31] A. Tsutsumi, Advanced IGCC/IGFC using exergy recuperation technology, Clean Coal Technol. J. 11 (2004) 17–22.
[32] J.-i. Hayashi, S. Hosokai, N. Sonoyama, Gasification of low-rank solid fuels with thermochemical energy recuperation for hydrogen production and power generation, Trans. IChemE 86 (B6) (2006) 409–419.
[33] M.G. Lussier, Z. Zhang, D.J. Miller, Characterizing rate inhibition in steam/hydrogen gasification via analysis of adsorbed hydrogen, Carbon 36 (1998) 1361–1369.
[34] B. Bayarsaikhan, N. Sonoyama, S. Hosokai, T. Shimada, J.-i. Hayashi, C.-Z. Li, T. Chiba, Inhibition of steam gasification of char by volatiles in a fluidized bed under continuous feeding of a brown coal, Fuel 85 (2006) 340–349.
[35] G. Guan, C. Fushimi, M. Ikeda, Y. Nakamura, A. Tsutsumi, T. Suda, M. Ishizuka, H. Hatano, S. Matsuda, Y. Suzuki, Flow behaviors in a high solid flux circulating fluidized bed composed of a riser, a downer and a bubbling fluidized bed, in: S.D. Kim, Y. Kang, J.K. Lee, Y.C. Seo (Eds.), Fluidization XIII: New Paradigm in Fluidization Engineering, Hotel Hyundai, Gyeong-ju, Korea, 2010, pp. 407–414.
[36] D. Bai, K. Kato, Quantitative estimation of solids holdups at dense and dilute regions of circulating fluidized beds, Powder Technol. 101 (1999) 183–190.
[37] H.W. Lei, M. Horio, A comprehensive pressure balance model of circulating fluidized beds, J. Chem. Eng. Jpn. 31 (1) (1998) 83–86.
[38] H. Chen, H. Li, S. Tan, Mechanism of achieving a dense downer: modeling and validation, Ind. Eng. Chem. Res. 45 (2006) 3488–3495.
[39] K. Kato, T. Takayuki, S. Hideki, T. Kazuhiko, The characteristic of fast fluidized bed, in: M. Kwauk, D. Kunii (Eds.), Fluidization'88: Science and Technology, Third China-Japan Symposium, Science Press, Beijing, 1988, pp. 130–136.

[40] H. Konno, S. Saito, Pneumatic conveying of solids though straight pipes, J. Chem. Eng. Jpn. 2 (1969) 211–217.
[41] B. Du, W. Warsito, L.-S. Fan, Behavior of the dense-phase transportation regime in a circulating fluidized bed, Ind. Eng. Chem. Res. 45 (2006) 3741–3751.
[42] H.-T. Bi, L.-S. Fan, Regime transition in gas-solid circulating fluidized beds, in: Proceedings of the AIChE Meeting, Los Angeles, CA, 1991 (Paper 101e).
[43] H.-T. Bi, J.R. Grace, Flow regime diagrams for gas-solid fluidization and upward transport, Int. J. Multiphase Flow 21 (1995) 1229–1236.
[44] U. Arena, A. Comomarota, L. Massimilla, L. Pistane, The hydrodynamic behavior of two circulating bed units of different sizes, in: P. Basu, J.F. Large (Eds.), Circulating Fluidized Bed Technology, vol. II, Pergamon Press, Toronto, 1988, pp. 223–230.
[45] R.M. Contractor, G.S. Patience, D.I. Garnett, H.S. Horowitz, G.M. Sisler, H.E. Bergna, A new process for n-butane oxidation to maleic anhydride using a circulating fluidized-bed reactor, in: A. Avidan (Ed.), Circulating Fluidized Bed Technology IV, AIChE, New York, 1994, pp. 387–391.